6 Production and Spectroscopy of Antihydrogen

C. Amsler, R. Brunner, D. Grögler, D. Lindelöf, H.P. Meyer, H. Pruys,
C. Regenfus, P. Riedler‡, J. Rochet‡, and T. Speer

in collaboration with:
CERN, Universities of Aarhus, Brescia, Genoa, Pavia, Tokyo, Wales,
Universidade Federal do Rio de Janeiro

(ATHENA Collaboration)

‡ presently at CERN, Geneva, Switzerland

6.1 Introduction

The final goal of the ATHENA experiment is to compare the properties of antihydrogen and hydrogen atoms with laser spectroscopic methods. In particular, we will measure the 1s - 2s energy difference in antihydrogen atoms. This will test CPT invariance for leptons and baryons with unprecedented accuracy, in the range 10^{-15} to 10^{-18}. Details on the project can be found in Refs. [1, 2] and in previous annual reports.

Antihydrogen has to be produced in large quantities for $\overline{\mathrm{H}}$ spectroscopy. The experimental programme has therefore been split into two distinct phases. The aim of the current phase 1 is to demonstrate the formation of antihydrogen in a Penning trap and to optimize the techniques needed to produce a cold antihydrogen gas. There are large uncertainties for the hydrogen formation rate. The plasma sizes and temperatures have to be controlled and varied, and various recombination schemes investigated. Particularly important are the antihydrogen formation rate as a function of plasma densities and electrode potentials, the recombination scheme, the fraction of antihydrogen atoms with kinetic energies below 0.1 meV, and the cross-section for annihilation with rest gas atoms. The actual CPT test, e.g. with lasers and stored antihydrogen atoms in an inhomogeneous magnetic field, is planned in phase 2 (after 2002). The eventual experimental approach to test CPT will depend on the results achieved during phase 1.

The apparatus consists of a superconducting solenoid (3 T) with a cold bore to house the antiproton trap, the positron storage trap, and the $\overline{\mathrm{H}}$ recombination trap. Antiprotons of 100 MeV/c from CERN's antiproton decelerator (AD) are injected along the axis of the magnet and are moderated through a silicon beam defining counter, an absorption foil and various windows. They are injected in a Penning trap (made of cylindrical electrodes) and reflected by an electrostatic potential. The $\bar{p}$ shot lasts for 200 ns (repetition rate of one every 2 minutes) after which the voltage of the entrance electrode is also raised to capture the antiprotons. They are then cooled to meV energies by interaction with a pre-loaded electron gas inside the capture trap.

Positrons from a strong ^{22}Na source are moderated in solid neon and transferred into a longitudinal magnetic field where they are moderated by nitrogen gas and electrostatic fields. They are then injected into a Penning trap similar to the one used to store the antiprotons, at the opposite end of the superconducting solenoid. The particles stacked in the two traps are finally transported to the central recombination trap which runs at a vacuum of 10^{-12} mbar.

In phase 1 the formation of antihydrogen will be demonstrated by detecting the *simultaneous* annihilation of the positrons (into two 511 keV γ's) and the antiprotons (e.g. into pions) which occurs when the unconfined (neutral) $\overline{\mathrm{H}}$ atoms hit the wall of the recombination trap. The detector to achieve this task has been proposed, developed and built by the University

of Zurich. It was assembled during 2000 and commissioned in autumn with the first beams from the AD. We now present the detector, discuss our recent R&D results with CsI crystals operating at low temperatures, and report on our experience with the first antiproton beams.

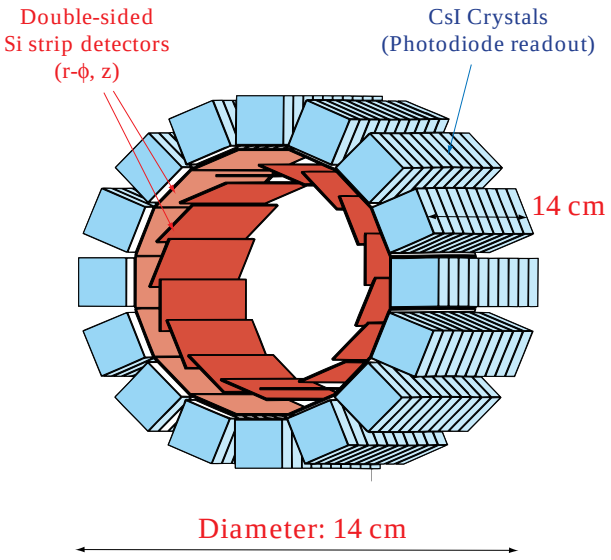

Figure 6.1: *3D sketch of the antihydrogen detector.*

6.2 Antihydrogen detector

The pions are detected in two layers of 16 silicon microstrip detectors, and the two back-to-back 511 keV photons in 16 layers of 12 pure CsI crystals (Fig. 6.1). The detector covers a solid angle of $0.85 \times 4\pi$ for charged annihilation particles and $0.66 \times 4\pi$ for γ detection. The unambiguous proof of antihydrogen formation will be obtained by searching for events for which the two hit crystals and the reconstructed annihilation vertex lie on a straight line. The detection of both photons and the collinearity test are important to reduce background: the main background is due to positrons from showers initiated e.g in the coils of the magnet by the high energy γ's of annihilation π^0's. The annihilation vertex can be determined from the charged tracks with an r.m.s. precision of 1.5 mm in radius and 3 mm along the axis. This is sufficient to establish that the events stem from annihilation of the neutral atoms hitting the wall of the recombination trap.

For best detection efficiency the detector is installed as close as possible to the recombination trap, inside the superconducting solenoid. The detector is located in a thermally insulated enclosure at the lowest temperature ($\simeq$ 77 K), at which the detector and read-out electronics can be operated. A number of technical problems (thermal expansions of the various detector components, temperature sensitivity of electronic components, light yield of CsI, etc) had therefore to be solved.

The support structure (see Fig. 6.2 right and last year's annual report) holding the outer silicon microstrip modules and the CsI crystals was machined from one block of aluminum in the mechanics workshop of our institute. The cylindrical wall was electro-eroded to 500 μm to minimize multiple scattering and γ conversions.

The two cylindrical layers of the double-sided silicon microstrip modules detect the charged pions stemming from an antiproton annihilation on the wall of the recombination trap, or with a rest gas atom (Fig. 6.2). The microstrip detectors were produced by SINTEF. They are 162 mm long, 19 mm wide and 380 μm thick and consist of two 81 mm long pieces (n-material) glued and bonded, building a module. The front side is divided into 384 p^+

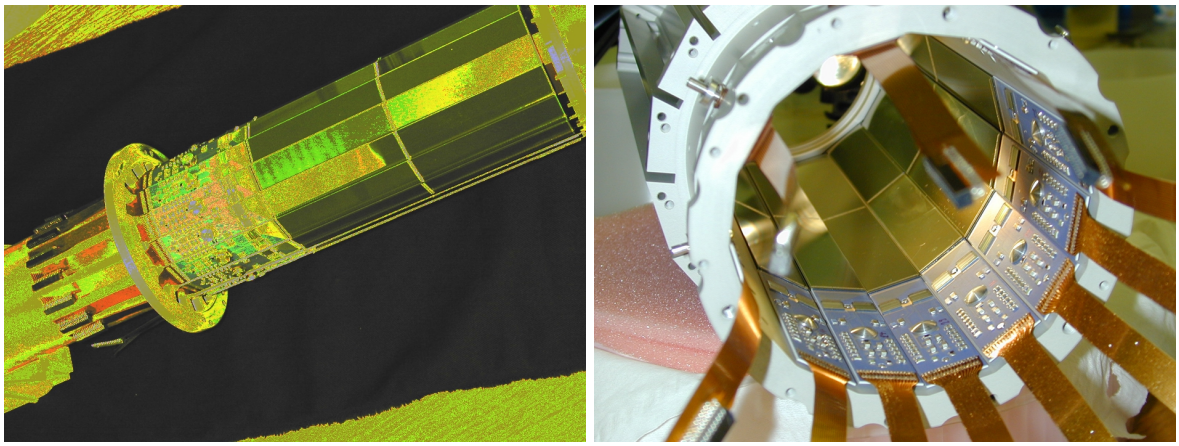

Figure 6.2: *Left: inner layer of 16 silicon microstrip modules, also showing the ceramic hybrids containing the preamplifiers and the capton readout cables. Right: outer layer of 16 silicon microstrip modules.*

strips with a pitch of 47 μm (measurement of the azimuthal angle ϕ), but every third strip only is connected to the readout electronics (hence 128 readout strips per module). The charge collected by the floating strips induces a signal on the readout strips by capacitive coupling. A multiple guard ring structure around the strips ensures low leakage current and a good stability against breakdown. The back side contains 64 pads with a pitch of 1.25 mm. The pads are oriented perpendicular to the strips (measurement of the z coordinate along the detector axis).

The modules are connected to VIKING type (VA2_TA) readout chips, modified for self-triggering and mounted with passive SMD electronics on a ceramic hybrid (see Fig. 6.2). The self-triggering VA2_TA chip is multiplexing its 128 channels into one analogue output line. The multilayered hybrids were designed by our group and built at CERN.

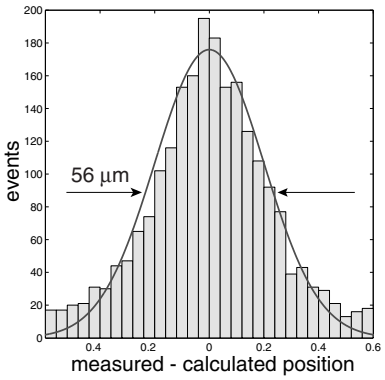

Figure 6.3: *Position resolution of the ATHENA test detector in strip units (140 μm).*

The signals are processed by analogue repeater cards (built by the electronics workshop of our institute) behind the vacuum flange and are then digitized by flash ADC's. The performance of the detector and the readout chips at 77 K was investigated with cosmic rays [3]. The position resolution was determined with our track defining silicon microstrip telescope [4]. Figure 6.3 shows the distribution of the difference between the coordinates predicted from the telescope and the coordinates measured with the ATHENA strips. The latter was derived from the mean strip number between the two signal strips, weighted by the energy deposits. The predicted coordinate was obtained from a linear fit to the hits in the beam telescope. We obtained an r.m.s. resolution of 24 μm (Fig. 6.3). The signal to

noise ratio was about 50.

The time resolution of the microstrip detector was also determined with cosmic rays and a resolution of 16 ns (FWHM) mas measured.

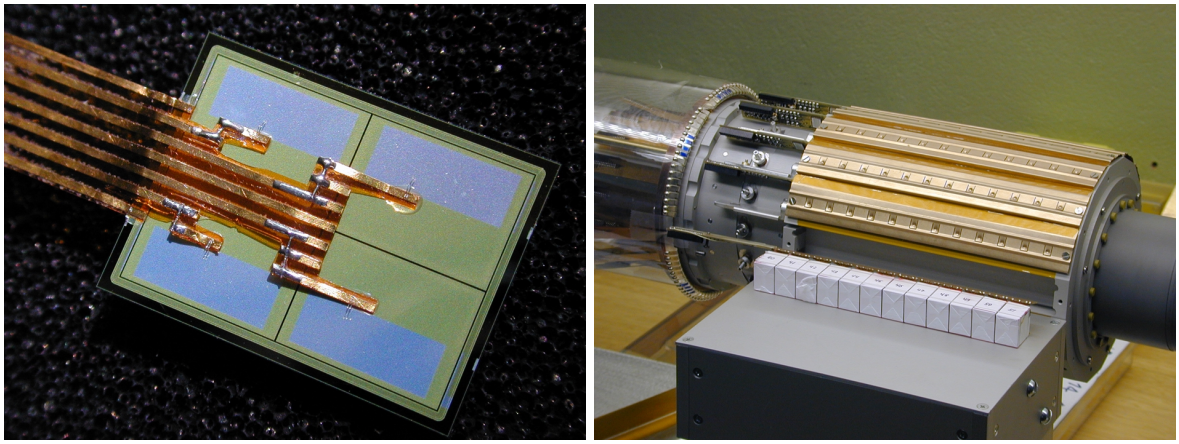

Figure 6.4: *Left: segmented photodiode with the bonded readout lines. The four (p^+) implants cover each a surface of 40 mm^2. Right: one of the 16 crystal rows before insertion into the support structure.*

The pure CsI crystals (manufactured by CHRISMATEC) are read out by photodiodes, also provided by SINTEF. As pure CsI emits light in the UV region, the diodes were especially designed with very thin entrance windows. Each photodiode was subdivided into four segments to reduce the capacitive noise (Fig. 6.4 left). The four pads were made of p^+ implants on n-material. The layer in contact with the crystal is a thin n^+ covered by a SiO_2 layer of thickness $\sim 0.75\ \lambda$ (where $\lambda = 350$ nm and 0.75 is the inverse of the refractive index), in an attempt to maximize the light reaching the depletion region. The positive voltage applied to the n^+ side is transferred to the guard ring on the pad side through an aluminum deposit along one edge of the diode.

The crystal dimensions are $13 \times 17.6 \times 17.1$ mm^3. Figure 6.4 right shows one of the 12 rows of crystals wrapped in teflon tape before insertion into the support structure.

The 48 readout lines of a crystal row (12×4 pads) are connected to one VA2_TA chip. Custom designed capton cables connect the 48 hybrids (2×16 for the 2 silicon layers and 16 for the crystals) with the patch panel (Fig. 6.5).

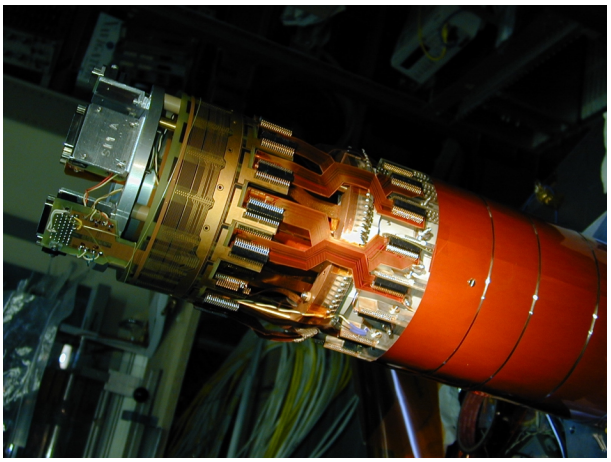

Figure 6.5: *Patch panel showing the readout side of the detector.*

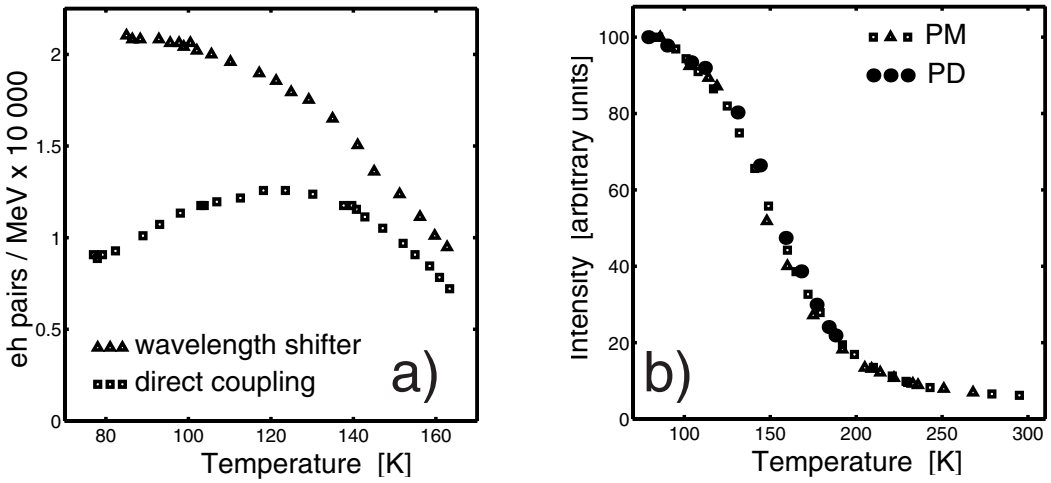

Figure 6.6: *a): Yield of electron-hole pairs measured with a pure CsI crystal and a photodiode, with and without wavelength shifter. b): Light yield of pure CsI crystals as a function of temperature. Both measurements, one with a photomultiplier (PM), and the other with a photodiode (PD) and wavelength shifter, are normalized independently to the maximum.*

6.3 Performance of undoped CsI at low temperature

In 1998 we initiated a programme to investigate the properties of pure CsI coupled to photodiodes as a function of temperature. We also built a test bench at 77 K to measure the light output with photomultipliers [5]. Tests with crystals from various suppliers using different polishing and wrapping methods were performed in parallel by our collaborators at Pavia.

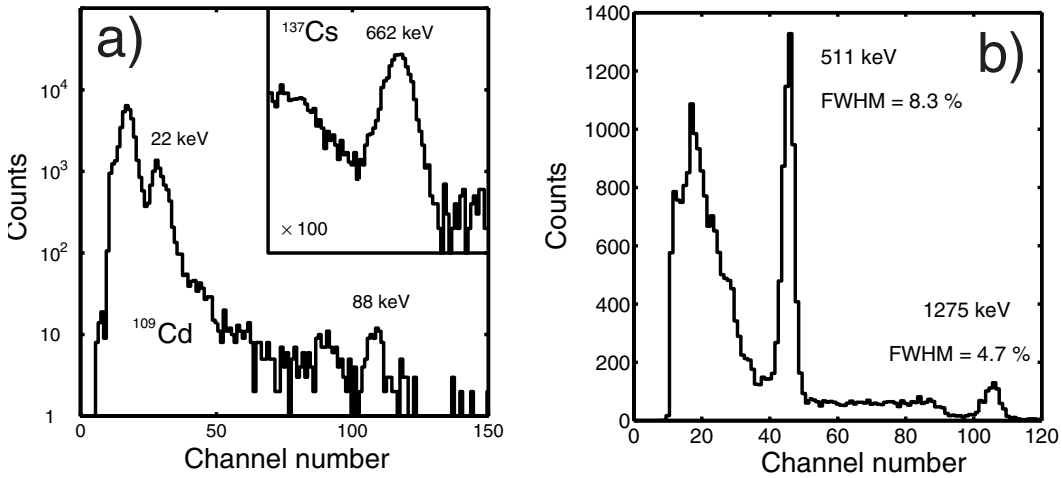

Figure 6.7: *a): Calibration of the photodiode at 77 K with X-rays from a ^{109}Cd source and γ-rays from a ^{137}Cs source (inset). b): ^{22}Na spectrum taken with a sprayed pure CsI crystal coupled to a photodiode and preamplifier at 77 K.*

Final results are being published [6]. The scintillation yield of pure CsI is known to increase with decreasing temperature. Hence the pulse height (proportional to the number of electron-hole pairs in the photodiode) was expected to behave accordingly. The increase in pulse height was indeed observed with photomultipliers, but with photodiodes we observed a maximum around 120 K, below which the signal decreased rapidly. This effect was traced

to the quantum efficiency of the photodiode which we measured as a function of wavelength, using a tunable light pulse generator (Xe lamp and diffractive grid) [7]. In the wavelength region of maximum light emission (340 nm at 77 K), the quantum efficiency of the photodiode oscillates between 10 and 20 % (presumably due to interference effects in the window), but rises rapidly above 360 nm to reach $\sim$ 75% at 600 nm. We therefore sprayed the faces of the crystal with a fluorescent red dye to shift the wavelength into the red range. The yields with and without paint are shown in Fig. 6.6a. The measurements with photomultiplier and photodiodes agree for red light (Fig. 6.6b) and the light output increases by a factor of 15.8 $\pm$ 1.0 between room temperature and 77 K.

The number of electron-hole pairs in the photodiode per unit energy deposit in the crystals was measured with the 662 keV photons from a ^{137}Cs source. The calibration was achieved with 22 and 88 keV X-rays from a ^{109}Cd source, directly absorbed in the photodiodes. Figure 6.7a shows the X-rays spectra. At 77 K we obtained 39'600 $\pm$ 1'200 electron-hole pairs per MeV, a result only 20 % below the yield of doped CsI(Tl) at room temperature. Figure 6.7b shows the γ spectrum from a ^{22}Na source. The resolution for 511 keV γ's is 8.3 % (FWHM). The decay time increases from 28 ns (main component) at 300 K to $\simeq$ 1 μs at 77 K [6]. The longer decay time is still acceptable for detecting antihydrogen in ATHENA.

6.4 First results with antiprotons

The antiprotons were decelerated in the AD from 3.5 GeV/c down to 100 MeV/c for the first time in July 2000 and the AD provided its first useful beam of 1.5 $\times$ 10^7 antiprotons per pulse at 100 MeV/c.

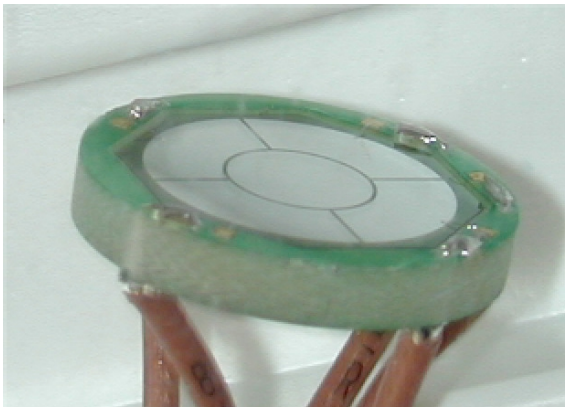

Figure 6.8: *Segmented silicon beam counter.*

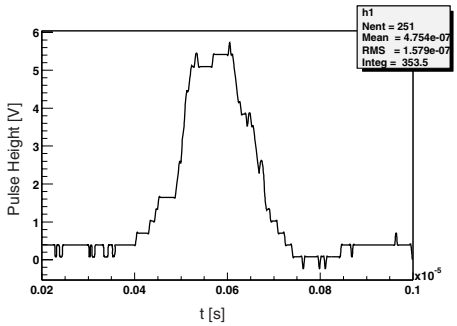

Figure 6.9: *Pulse height delivered by the silicon beam counter; the spill length is about 200 ns and corresponds to a few 10^6 antiprotons.*

The first thousand trapped antiprotons were also observed in ATHENA in July 2000. The extracted beam had a diameter of 3 mm and a momentum bite $\Delta p/p$ of 10^{-4}. The current from the incident antiprotons was measured in front of the $\bar{p}$ capture trap. Figure 6.8 shows the segmented silicon counter that was recycled from our former Crystal Barrel experiment. The segmentation allowed a fine steering of the incident beam. Figure 6.9 shows the current as a function of time. An intensity of typically 3 $\times$ 10^6 antiprotons per pulse could be derived from the measured current. The noise induced on the beam counter by the nearby quickly rising trapping voltage was found to be negligible (typically 100 mV compared to a $\bar{p}$ signal of several volts, see Fig. 6.9).

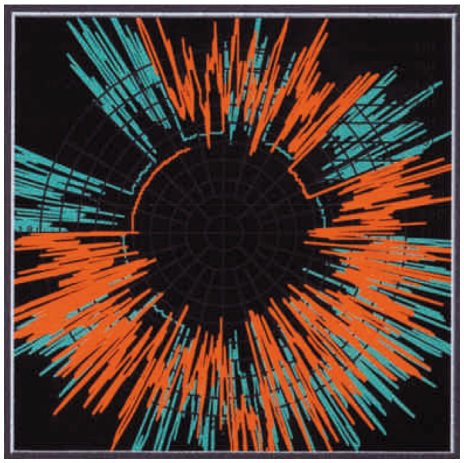

Figure 6.10: *Signals from annihilation pions in the detector inner layer (red) and outer layer (blue). The lengths of the spikes are proportional to the energy losses.*

The antiprotons were degraded by an aluminium foil and then electrostatically decelerated in the trap. Figure 6.10 shows pion tracks in the microstrip detector from a spill of antiprotons annihilating in the entrance windows. A thin rotating foil allowed for fine tuning of the absorber material needed to capture the antiprotons. The optimum degrader thickness was found by counting the stored antiprotons through their delayed annihilation: The voltage on the entrance electrode, which had been raised at the end of the spill, was lowered slowly. This allowed the antiprotons to escape the trap and to annihilate in the apparatus. The rate was measured by scintillator paddles installed below the magnet. Figure 6.11 shows the $\bar{p}$ annihilation rate as a function of time for various absorber thicknesses, and also the final range curve. The estimated total number of trapped antiprotons was around 7,000 per spill in these first attempts.

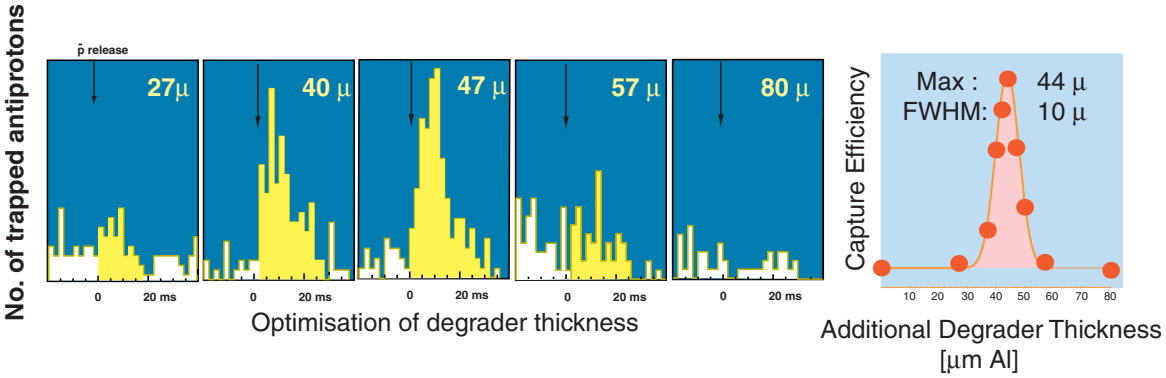

Figure 6.11: *Annihilation from antiprotons escaping the trap as a function of time (during the slow reduction of the confining voltage) for different beam degrader thicknesses. The number of trapped antiprotons reaches a maximum around 44 μm of aluminium (right curve).*

Once captured, the antiprotons could be cooled to meV energies by an electron gas. This cold gas (typically 3×10^8 electrons) was preloaded in the trap with an additional electrostatic potential supplied by the central ring electrodes (Fig. 6.12). Electron cooling occurs rapidly by synchrotron radiation. The cooled antiprotons can be detected by first reducing the main trapping voltage T_1 (which elimates the hot antiprotons) and then the additional well T_2 (which eliminates the cold antiprotons). Figure 6.12 is quite encouraging as it demonstrates that indeed the number of cool antiprotons increases with cooling time.

Summarizing, the ATHENA experiment and the AD perform as expected. Initial trials

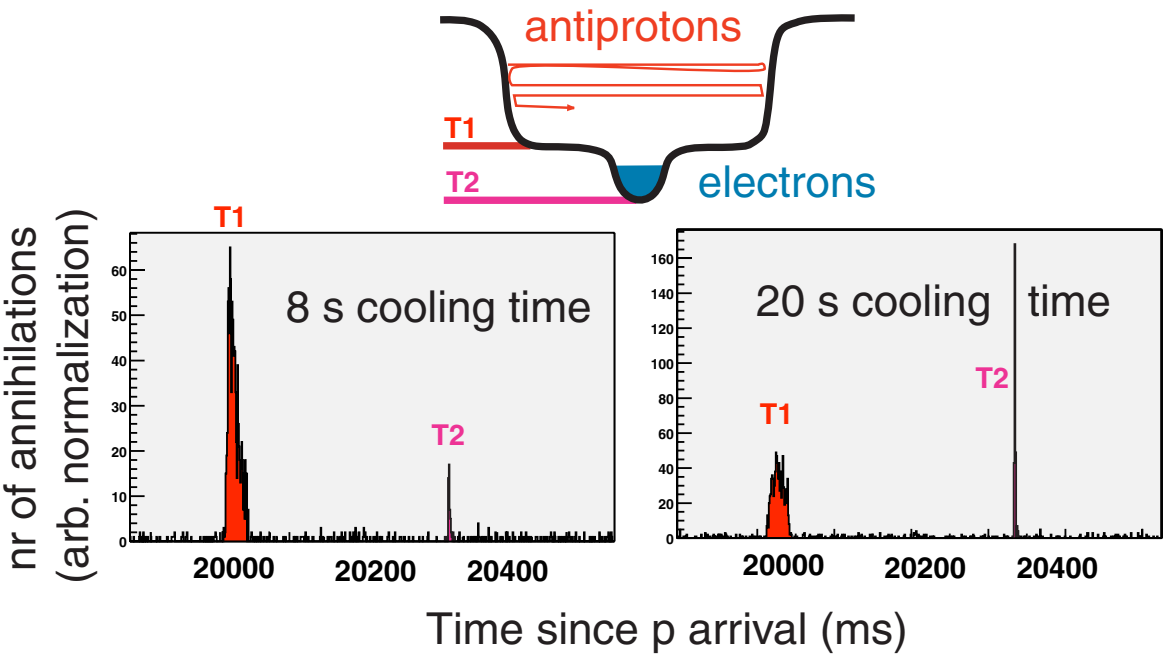

Figure 6.12: *Annihilation rate, showing that the fraction of electron cooled antiprotons T_2 increases with time (see text).*

to capture protons and positrons are quite promising. Our goal for the next two years is to demonstrate the formation of antihydrogen and to optimize the $e^+\bar{p}$ recombination rate.

References

[1] ATHENA proposal, CERN SPSLC 96-47, see http://www.cern.ch/athena/

[2] C. Amsler et al. (ATHENA Collaboration), Proc. Hydrogen II Conf., Castiglione de Pescaia, Springer (2000)

[3] R. Brunner, *Aufbau und Test eines Microstrip-Detektors für das ATHENA-Experiment*, Diplomarbeit, Universität Zürich, 2000

[4] C. Amsler et al., Submitted to Nucl. Instr. and Methods in Phys. Res.

[5] P. Niederberger, *Untersuchung von CsI-Szintillatoren bei tiefen Temperaturen*, Diplomarbeit, Universität Zürich, 1999

[6] C. Amsler et al., Submitted to Nucl. Instr. and Methods in Phys. Res.

[7] We thank the IPHE group for the kind assistance during these measurements at Lausanne University